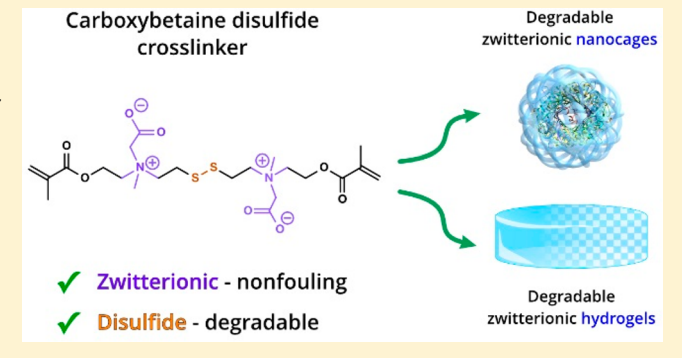
Zwitterionic Hydrogels Based on a Degradable Disulfide Carboxybetaine Cross-Linker

Priyesh Jain,^{†,§} Hsiang-Chieh Hung,^{†,§} Bowen Li,[‡] Jinrong Ma,[†] Dianyu Dong,[†] Xiaojie Lin,[†] Andrew Sinclair,[†] Peng Zhang,[†] Mary Beth O'Kelly,[†] Liqian Niu,[†] and Shaoyi Jiang**,^{†,‡}

[†]Department of Chemical Engineering and [‡]Department of Bioengineering, University of Washington, Seattle, Washington 98195, United States

ABSTRACT: We report the synthesis of a zwitterionic carboxybetaine disulfide cross-linker (CBX-SS) and biodegradable poly(carboxybetaine) (PCB) hydrogels and nanocages (NCs) made using this cross-linker. The structure of CBX-SS combines zwitterionic carboxybetaine to confer nonfouling properties and a disulfide linkage to facilitate degradation. The physical, mechanical, and fouling characteristics of PCB hydrogels cross-linked with CBX-SS were investigated. Then, the degradation characteristics of CBX-SScross-linked hydrogels were evaluated through their weight loss and release of an encapsulated protein in a reducing environment. Furthermore, CBX-SS was applied to prepare degradable PCB NCs. Results show that encapsulating the



highly immunogenic enzyme uricase in degradable PCB NCs eliminates or prevents an in vivo immune response to both the protein and polymer.

1. INTRODUCTION

Zwitterionic polymers such as phosphobetaine, sulfobetaine, and carboxybetaine³⁻⁶ have attracted significant interest in recent years for a variety of applications such as medical implants, wound healing dressings, tissue scaffolds, drug delivery carriers, membranes, biosensors, consumer products, and marine coatings. These polymers have emerged as a unique class of biomaterials due to their superior nonfouling capabilities, as they are highly resistant to nonspecific biomolecular adsorption and microorganism attachment to surfaces. Zwitterionic materials derive their antifouling nature from strong hydration layers that form around the opposing charges at the zwitterionic centers. Among all zwitterionic materials known, polycarboxybetaine (PCB) polymers are unique due to their combination of ultralow fouling properties, functionalization potential, and charge-switching abilities. Recently, PCB hydrogels have been shown to resist collagenous encapsulation and inhibit the foreign body response upon subcutaneous implantation in mice.8 In addition, PCB hydrogels maintain the multipotency of encapsulated stem cells and mitigate nonspecific cell differentiation. The superior performance of PCB hydrogels in complex biological environments can be attributed to their composition; they are formed from PCB monomers along with CBX, 10,11 a zwitterionic CB cross-linker that contributes to their excellent nonfouling properties. In addition, unlike many commercial cross-linkers, CBX is highly soluble in water. However, PCB hydrogels cross-linked with CBX are not

biodegradable. Degradable hydrogels are highly desirable for many applications from drug delivery to tissue engineering.

In this work, we focused on making a degradable zwitterionic CB cross-linker. Polymers can be designed to degrade via ester hydrolysis, disulfide cleavage, enzymatic hydrolysis, photolytic cleavage, or a combination of these mechanisms. The incorporation of a disulfide linkage is a particularly popular strategy for making degradable crosslinkers. We designed and synthesized the degradable CB crosslinker reported here, CBX-SS, from 2-hydroxyethyl disulfide. Consisting of both nonfouling zwitterionic CB units and disulfide linkages, CBX-SS provides degradable sites that can be cleaved by a biological reducing agent such as glutathione (GSH), DL-dithiothreitol (DTT), or cysteine 13,14 via thioldisulfide exchange reactions at a time scale from minutes to hours. This rapid cleavage is distinct from hydrolytically degradable bonds such as ester and carbonate bonds which usually exhibit gradual degradation kinetics inside the body at a time scale from days to months.

To evaluate this degradable zwitterionic CB cross-linker, we prepared degradable PCB/CBX-SS hydrogels over a wide range of cross-linker concentrations, from 5 up to 100%. We then encapsulated fluorescein isothiocyanate-labeled BSA

Special Issue: Zwitterionic Interfaces: Concepts and Emerging Applications

Received: June 20, 2018 Revised: August 15, 2018 Published: August 17, 2018

(FITC-BSA) inside PCB/CBX-SS hydrogels as a model drug and tracked its release rate using DTT as a cleaving agent. Additionally, we used this cross-linker to synthesize degradable PCB NCs for protein encapsulation. Our results demonstrate that these degradable PCB NCs have similar performance to a nondegradable version and improve the pharmacokinetics (PK) while mitigating the immunological properties of uricase, a highly immunogenic enzyme.

2. EXPERIMENTAL METHODS

2.1. Materials. *p*-Toluenesulfonyl chloride (*p*-TsCl), 2-hydroxyethyl disulfide, triethylamine (TEA), 2-(methylamino)ethanol, methacryloyl chloride, ammonium persulfate (APS), *N*,*N*,*N*',*N*'-tetramethylethylenediamine (TEMED), and dithiothreitol (DTT) were purchased from Sigma-Aldrich (St. Louis, MO). *tert*-Butyl bromoacetate was purchased from Oakwood Chemicals (West Columbia, SC), and trifluoroacetic acid (TFA) was purchased from TCI America (Portland, OR). Ethyl acetate, hexane, dichloromethane (DCM), methanol, and IRN-78 resin were purchased from Fisher Scientific (Hampton, NH). Thin layer chromatography (TLC) was performed on glass plates (Whatman) coated with 0.25 mm of silica gel (60 Å, 70–230 mesh). All ¹H and ¹³C NMR spectra were recorded on a Bruker 500 MHz spectrometer in CDCl₃ unless otherwise specified, and chemical shifts are reported in ppm (δ) relative to the internal standard, tetramethylsilane (TMS).

2.2. Synthesis of a Degradable CBX-SS Cross-Linker. *2.2.1. Synthesis of Disulfanediylbis(ethane-2,1-diyl)bis(4-methylbenzenesulfonate)* (2). A solution of *p*-toluenesulfonyl chloride (59.2 g, 310.5 mmol) in 100 mL of dichloromethane was added dropwise to a stirred solution of 2-hydroxyethyl disulfide (20 g, 129.6 mmol) and triethylamine (43.2 g, 427.1 mmol) in 200 mL of dichloromethane at 0 °C. The reaction mixture was allowed to warm to room temperature and was stirred for 6 h. The reaction mixture was then washed with sat. NaHCO₃ (2 × 200 mL) and water (2 × 150 mL). The organic layer was dried using sodium sulfate, filtered, and concentrated in vacuo to leave a thick viscous oil. The crude product was then crystallized using ethyl acetate/hexane (10:90) to give compound 2 as a white powder in 86.3% yield. ¹H NMR (500 MHz, CDCl₃) δ 7.80 (d, J = 8.3 Hz, 4H), 7.36 (d, J = 8.0 Hz, 4H), 4.21 (t, J = 6.7 Hz, 4H), 2.85 (t, J = 6.7 Hz, 4H), 2.46 (s, 6H).

2.2.2. Synthesis of 2,2'-((Disulfanediylbis(ethane-2,1-diyl))bis-(methylazanediyl))bis(ethan-1-ol) (3). Compound 2 (49 g, 105.9 mmol) was dissolved in 400 mL of acetonitrile, and K_2CO_3 (36.75 g, 265.8 mmol) was added. After 5 min, 2-(methylamino)ethanol (39.69 g, 528.4 mmol) in 40 mL of acetonitrile was added to the suspension at room temperature. The reaction contents were stirred for 48 h at room temperature until TLC indicated complete consumption of the starting material. After reaction completion, a white solid was filtered off using filtration aid Celite. The reaction mixture was concentrated to dryness in vacuo and further purified by column chromatography to give compound 3 in 90.5% yield. ¹H NMR (500 MHz, CDCl₃) δ 3.63–3.59 (m, 4H), 2.85 (t, J = 6.7 Hz, 4H), 2.75 (t, J = 6.9 Hz, 4H), 2.59–2.56 (m, 4H), 2.30 (s, 6H).

2.2.3. Synthesis of ((Disulfanediylbis(ethane-2,1-diyl))bis(methylazanediyl))bis(ethane-2,1-diyl)bis(2-methylacrylate) (4). A solution of methacryloyl chloride (6.54 mL, 66.9 mmol) in 20 mL of DCM was added dropwise to a solution of compound 3 (6.0 g, 22.3 mmol) and TEA (9.12 mL, 67.0 mmol) in 40 mL of DCM at 0 °C over a period of 20 min. The reaction mixture was allowed to warm to room temperature and was stirred for 2 h. The reaction mixture was then washed with sat. NaHCO₃ (2 × 30 mL), water (1 × 30 mL), and brine (1 × 30 mL). The organic layer was dried using sodium sulfate, filtered, and concentrated in vacuo to leave a residue which was further purified by column chromatography to give compound 4 in 85.1% yield. ¹H NMR (500 MHz, CDCl₃) δ 6.12 (s, 2H), 5.57 (s, 2H), 4.27 (s, 4H), 2.80 (d, J = 14.2 Hz, 12H), 2.37 (s, 6H), 1.95 (s, 6H).

2.2.4. Synthesis of N,N'-(Disulfanediylbis(ethane-2,1-diyl))bis(2-(tert-butoxy)-N-(2-(methacryloyloxy)ethyl)-N-methyl-2-oxoethan-

1-aminium) Bromide (5). Compound 4 (5.5 g, 13.6 mmol) was dissolved in 30 mL of acetonitrile, and then tert-butyl bromoacetate (6.0 mL, 40.7 mmol) was added. The reaction contents were stirred for 18 h at 56 °C until TLC showed complete consumption of the starting materials. The reaction mixture was concentrated to dryness in vacuo. A mixture of hexane/ethyl acetate (1:1) (2 × 30 mL) was added to the viscous residue, and the resulting solution was stirred for 15 min. After 15 min, the supernatant liquid was decanted, and diethyl ether (1 × 40 mL) was added. The solution was stirred for 1 h to give compound 5 as a white solid in 85.2% yield. ¹H NMR (500 MHz, CDCl₃) δ 6.17 (d, 2H), 5.67 (d, 2H), 4.76–4.61 (m, 8H), 4.53–4.17 (m, 8H), 3.89–3.61 (m, 10H), 1.96 (s, 6H), 1.53 (s, 18H).

2.2.5. Synthesis of 10-(Carboxylatomethyl)-3-(2-(methacryloyloxy)ethyl)-3,10,15-trimethyl-14-oxo-13-oxa-6,7-dithia-3,10-diazahexadec-15-en-3,10-diiumoate [CBX-SS] (6). Compound 5 (1.8 g, 2.3 mmol) was taken up in 15 mL of DCM, and then 15 mL of TFA was added to it. After complete cleavage of the tertbutyl protecting group, the reaction mixture was concentrated in vacuo. The residual mixture was dissolved in 30 mL of water, IRN-78 resin was added for neutralization, and then the mixture was subjected to lyophilization on a freeze-dryer to give compound 6 in 93.1% yield. $^1\mathrm{H}$ NMR (300 MHz, D₂O) δ 6.07 (s, 2H), 5.68 (s, 2H), 4.63–4.51 (m, 4H), 4.16 (s, 4H), 4.12–3.83 (m, 8H), 3.53–3.41 (m, 4H), 3.24 (s, 6H), 1.83 (s, 6H).

2.3. Hydrogel Preparation. PCB/CBX-SS hydrogels were fabricated by bulk polymerization. The hydrogel reactant solution was prepared in phosphate-buffered saline (PBS), with the total concentration of carboxybetaine acrylamide (CBAA)¹⁰ monomer and CBX-SS cross-linker fixed at 2.6 M. Different formulations were made by substituting the monomer for the cross-linker in increasing amounts; 5, 10, 15, 30, and 100% by mole. The 100% cross-linker hydrogels were made from 2.6 M solutions of the cross-linker. Polymerization was initiated by adding APS/TEMED (0.1 M/0.66 M) to the hydrogel solution, which was placed between two glass slides separated by 1 mm-thick polytetrafluoroethylene spacers and polymerized at room temperature for 2 h. After polymerization, hydrogels were removed from the casts and soaked in PBS for 3 days to remove unreacted chemicals and neutralize the hydrogel network. PBS was refreshed every 12 h.

2.4. Swelling and Mechanical Characterization of Hydrogels. After soaking in PBS for 3 days, the fully swollen hydrogel disks were weighed and then dehydrated at 60 °C under vacuum (30 in. Hg) for 3 more days. Dried hydrogel disks were weighed. The equilibrium water contents (EWC) were calculated by the following equation

$$EWC = 100(\%) \frac{m_{\rm s} - m_{\rm d}}{m_{\rm s}}$$
 (1)

where m_s is the mass of the fully swollen hydrogel and $m_{\rm d}$ is the mass of the dry hydrogel.

To measure the mechanical properties of the hydrogels, compressive tests were performed using a compressive mechanical tester (Instron 5543A, Instron Corp., Norwood, MA) with a 10 kN load cell. Biopsy punches were used to punch hydrated hydrogels into 5 mm-diameter disks. The crosshead speed was set at 1 mm/min. Average data were acquired by testing three specimens for each sample.

Dynamic rheological behaviors of the hydrogels were tested with a rotational rheometer (Physica MCR 301, Anton Paar, Austria) using 25 mm parallel plate geometry and a 1 mm gap. Hydrogels varying in cross-linker amount (5, 10, and 15% by mole) were fully swollen in PBS, and the storage modulus (G') and loss modulus (G'') were recorded over a strain sweep from 0.1 to 100% strain (oscillation frequency of 1 rad/s, 25 °C).

2.5. Protein Adhesion by Enzyme-Linked Immunosorbent Assay (ELISA). Biopsy punches were used to punch fully swollen hydrogels into 5 mm-diameter disks. Hydrogel disks were then placed into wells of a 24-well plate and incubated with 1 mL of human fibrinogen (1 μ g/mL) in PBS for 1 h. All samples were then transferred to new wells after five washes with pure PBS. After this, all

Scheme 1. Synthesis of a Biodegradable CBX-SS Cross-Linker

samples were incubated in 1 mL of horseradish peroxidase (HRP) conjugated antifibrinogen (0.1 μ L/mL) in PBS for 1 h and washed with PBS in new wells as before. Next, 1 mL of 1 mg/mL o-phenylenediamine (OPD) in 0.1 M citrate phosphate (pH 5.0) solution containing 0.03% hydrogen peroxide was added. After incubation for 15 min, the enzymatic reaction was stopped by adding an equal volume of 1 N HCl. The absorbance at 492 nm was recorded by a plate reader (Cytation 3, BioTek, Winooski, VT).

2.6. Hydrogel Degradability. To test degradability, hydrated PCB/CBX-SS hydrogels of different cross-linker amounts were soaked in a PBS solution containing DTT at room temperature. A high concentration of 100 mM DTT solution was used for fast degradation. The weight change $[100\%(W_d/W_e)]$ with respect to degradation time was recorded; W_d denotes the weight of the hydrogel after a selected incubation time, and W_e denotes the weight of the original hydrogel.

2.7. In Vitro Drug Release. FITC-conjugated bovine serum albumin (FITC-BSA) was loaded into a bulk hydrogel (10 mol % CBX-SS) produced with the above protocol, with selected amounts of FITC-BSA added to the precursor solution. The precursor mixture was injected into the gap between two glass slides separated by a 0.5 mm-thick polytetrafluoroethylene spacer and then allowed to polymerize for 2 h at room temperature. Uniform FITC-BSA-loaded hydrogel disk samples of 5 mm in diameter were fabricated using a biopsy punch. The initial amount of FITC-BSA loaded per disk was calculated to be 84 μ g. For release testing, disk samples were immersed in 5 mL of DTT solution (0, 5, or 20 mM) in PBS and rotated on a rotary mixer at room temperature. To obtain the release profile, 60 μ L of the release solution was withdrawn and then replaced by 60 μ L of fresh corresponding solution at regular time points. The cumulative release amount of FITC-BSA was measured by the fluorescence intensity of release solution using a microplate reader (ex = 494 nm, em = 520 nm) and calculated using the following equation (each measurement was performed in triplicate)

cumulative release (%) =
$$\frac{5C_n + 0.06 \sum C_{n-1}}{84} \times 100$$
 (2)

where C_n and C_{n-1} are the FITC-BSA concentrations (μ g/mL) in the release solution withdrawn n and n-1 times, respectively, which was

recalculated from the corresponding fluorescence intensity and the standard curve.

2.8. Synthesis of Degradable PCB/CBX-SS Nanocages (NCs). PCB/CBX-SS nanocages were synthesized according to our previously reported protocol. 15 Briefly, AOT (sodium bis(2-ethylhexyl) sulfosuccinate, 237 mg) and Brij 30(poly(ethylene glycol) dodecyl ether, 459 mg) were added to a 20 mL glass vial containing a stir bar. The glass vial was sealed with Teflon tape and purged with dry nitrogen for 10 min. Nitrogen-deoxygenated hexane (10 mL) was then slowly added to the vial under vigorous stirring. For the aqueous phase, uricase (2 mg) was dissolved in HEPES buffer (pH 8.5, 250 μ L), and CBAA (40 mg) and CBX-SS (10 mg) were added. Dry nitrogen was then bubbled through the monomer/protein solution for 2 min, after which the aqueous phase was slowly added dropwise to the organic phase. The vial was then sonicated to form a microemulsion. A 20% (w/v) solution of ammonium persulfate in deionized water (10 μ L) was then added to the emulsion, and after 5 min, tetramethylethylenediamine (TEMED, 6 µL) was added to initiate polymerization. The reaction contents were maintained at 4 °C under rapid magnetic stirring. After a 2 h reaction time, the organic solvent was removed using a rotary evaporator, and the desired nanocages were precipitated and washed with THF three times. Nanocages were then resuspended in PBS and purified with 300 kDa molecular weight cutoff centrifugal filters to remove any free uricase protein.

2.9. Pharmacokinetics and Immunogenicity Studies. All animal experiments adhered to federal guidelines and were approved by the University of Washington Institutional Animal Care and Use Committee (IACUC). Spraque-Dawley rats (male, body weight 74-100 g) were obtained from Jackson Laboratories (Seattle, WA). Rats were randomized into two groups at the beginning of each study (three animals per group). Native uricase and PCB-uricase nanocage samples were administered to the rats via tail vein injection at the dose of 25 U/kg body weight. Blood samples were collected from the tail vein 5 min and 3, 12, 24, 48, and 72 h after the injection. The blood samples were put in heparinized vials and centrifuged, and the enzyme content in plasma was estimated by enzyme activity. The circulation half-life of each uricase sample was calculated using PKSolver following the instructions. Three weeks after the injection, 5 mL of blood was drawn by cardiac punch, and serum was prepared for antibody detection. Rat sera collected at the end of the animal study

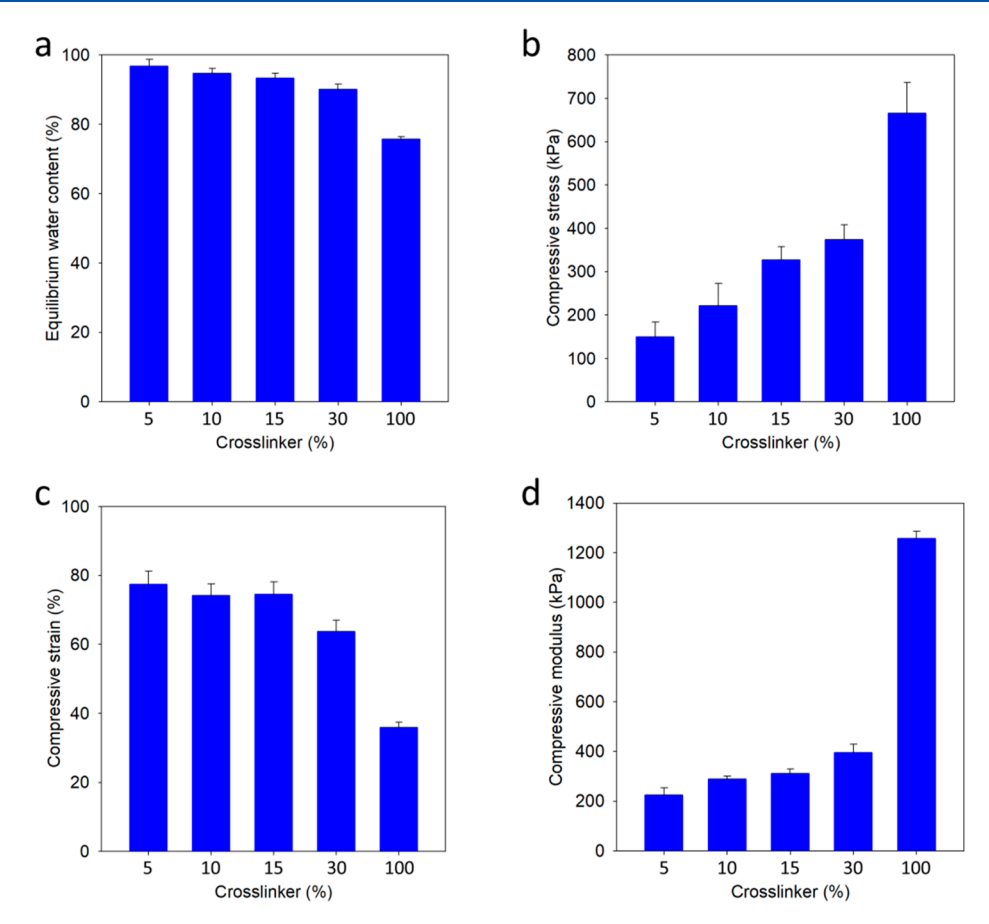


Figure 1. (a) Equilibrium water content of PCB/CBX-SS hydrogels with cross-linker contents of 5, 10, 15, 30, and 100% by mole; (b-d) Fracture compressive stress, fracture compressive strain, and compressive modulus of PCB/CBX-SS hydrogels with cross-linker contents of 5, 10, 15, 30, and 100% by mole, respectively.

(21st day) was handled for an ELISA test following the protocol we previously reported. $^{16}\,$

3. RESULTS AND DISCUSSION

3.1. Synthesis of CBX-SS Cross-Linker. Previously, our group introduced a zwitterionic CB cross-linker, CBX, which we have used extensively to make pure zwitterionic hydrogels.¹¹ While this cross-linker gives PCB hydrogels excellent nonfouling properties, it is not amenable to degradation, which is highly desirable for many applications. The addition of a disulfide group to the CB cross-linker is one way to introduce degradability. Most known disulfide cross-linkers are hydrophobic, which would hamper the nonfouling properties of zwitterionic hydrogels. To the best of our knowledge, no crosslinker possessing both nonfouling and degradable properties exists. Thus, we designed the CBX-SS cross-linker to combine nonfouling characteristics via its zwitterionic moiety with degradability via a disulfide bond. These disulfide bonds can be easily cleaved with reducing agents such as cysteine, dithiothreitol (DTT), and glutathione (GSH). It is generally challenging to synthesize cross-linkers and even more difficult if a highly polar zwitterionic moiety is introduced. To overcome these difficulties in this work, we designed a scheme to synthesize a CBX-SS cross-linker from 2-hydroxyethyl disulfide as shown in Scheme 1. Here, the tosylation of 2hydroxethyl disulfide 1 with tosyl chloride gave ditosylated compound 2, which undergoes nucleophilic substitution with N-methyl ethanolamine to give symmetrical disulfide 3 with

tertiary amino groups and terminal hydroxyl groups. This reaction takes about 2 days to reach completion, as monitored by TLC. Further reaction of symmetrical disulfide 3 with methacryloyl chloride forms bismethacrylate esters 4 of a symmetrical disulfide having tertiary amine groups. The zwitterionic carboxybetaine moieties are then introduced by performing N-alkylation of compound 4 with tert-butyl bromoacetate to form tert-butyl protected CBX-SS cross-linker 5. Acidic hydrolysis of compound 5 with TFA/DCM gives CBX-SS cross-linker 6 in acidic form. This compound can be easily crystallized out using methanol/diethyl ether. The crosslinker can be stored in the acidic form for a prolonged period of time and can be neutralized with IRN-78 resin to switch to its zwitterionic form. Using this scheme, a CBX-SS cross-linker can be easily synthesized on a large scale. Notably, the entire synthesis procedure involves only one flash column chromatography step, conserving time and solvent and improving efficiency.

3.2. Swelling and Mechanical Properties of PCB/CBX-SS Hydrogels. The high water content of hydrogels, resembling that of biological tissues, allows them to be used for biological applications. Equation 1 is used to calculate the equilibrium water content of hydrogels. Figure 1a shows the equilibrium water content measured for CBX-SS-cross-linked PCB hydrogels from 5% CBX-SS to 100% CBX-SS. As expected, an increase in the CBX-SS cross-linker content results in a decrease in water content. However, even for 100% CBX-SS-cross-linked hydrogels, the equilibrium water content

is around 75%, which is remarkably high for such a high degree of cross-linking.

In general, increased hydration weakens the mechanical strength of hydrogels, and this is a common challenge faced by highly hydrated zwitterionic hydrogels. 17,18 To mimic biological tissues and create an environment conducive to cell growth, hydrogels should be soft but have enough mechanical strength to keep the scaffold intact. As shown in Figure 1b,c, as we increased the molar percentage of cross-linker from 5 to 100%, the resulting PCB/CBX-SS hydrogels became more rigid but relatively more fragile. However, it is noteworthy how well the highly hydrated PCB/CBX-SS hydrogels maintained their mechanical strength. Figure 1d shows the compressive Young's moduli of the hydrogels; a 5% cross-linker content resulted in hydrogels with a high modulus of around 200 kPa, and greater cross-linker levels produced gels with moderately higher moduli. At a cross-linker content of 100% (pure CBX-SS hydrogels), the modulus reached around 1.2 MPa, which is impressive for a material with an equilibrium water content of 76%. Overall, the mechanical properties of PCB/CBX-SS hydrogels can be easily tuned for the desired application.

3.3. Protein Adsorption onto PCB/CBX-SS Hydrogels. Fibrinogen is a blood protein that adsorbs readily onto numerous surfaces via nonspecific interactions. This fibrinogen adsorption is commonly quantified by an enzyme-linked immunosorbent assay (ELISA) method, as was done in this work. After allowing complete swelling in PBS, PCB hydrogels prepared with 5, 10, 15, 30, and 100% CBX-SS cross-linker were incubated in human fibrinogen solutions to test their nonfouling properties. We hypothesized that PCB/CBX-SS hydrogels would be nonfouling at both low and high cross-linker contents. As shown in Figure 2, regardless of the cross-linker content, all PCB/PCBX-SS hydrogels exhibited excellent nonfouling properties. Tissue culture polystyrene (TCPS) was used as a positive control.

3.4. Degradability of PCB/CBX-SS Hydrogels. In tissue engineering, scaffolds used for tissue regeneration are designed to provide transient support. Therefore, the ability to tune hydrogel degradation to match the rate of tissue formation is

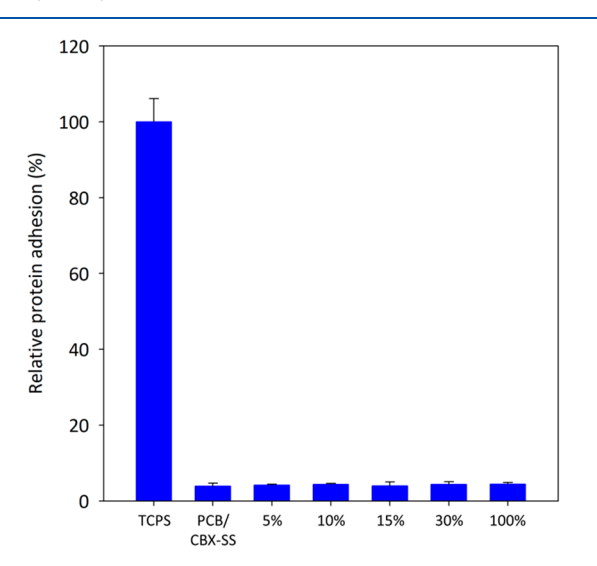


Figure 2. HRP-conjugated antifibrinogen adhesion on the PCB/CBX-SS hydrogels with cross-linker contents of 5, 10, 15, 30, and 100% by mole. TCPS and PCB/CBX-SS hydrogels were used as positive and negative controls, respectively.

highly desirable. During degradation, hydrolytically or enzymatically susceptible linkages are broken; when certain linkages break, mass is eroded from the hydrogel. To study the degradation of PCB/CBX-SS hydrogels in vitro, we measured the mass loss of CBX-SS-cross-linked hydrogels incubated in 100 mM DTT solution. Figure 3a shows the relative mass $[100\%(W_d/W_e)]$ of PCB/CBX-SS hydrogels after specified degradation times using 100 mM DTT as a reducing agent. As disulfide linkages are cleaved, the mass decreases until there are no longer a sufficient number of cross-links to hold the network together, at which point the remaining highly branched chains collapse and dissolve. The hydrogel with 5 mol % cross-linker degraded rather quickly, which may have been due to its weak support structure and low polymer content. All other hydrogels first showed an increase in mass as some of the disulfide linkages were cleaved, weakening the gel and allowing further swelling before they dissolved completely. As expected, the hydrogels with the lowest degrees of crosslinking degraded the most quickly in the presence of DTT, whereas hydrogels with higher cross-linker contents had comparatively increased stability toward responsive degradation. Figure 3b shows the representative degradation of hydrated PCB/CBX-SS hydrogels with 15 mol % cross-linker, where a higher concentration of the hydrogel-dissociation medium (500 mM DTT in PBS) was used.

3.5. In Vitro Drug Release Behavior of PCB/CBX-SS **Hydrogels.** Disulfide linkages can be easily cleaved by various reducing agents, such as DL-dithiothreitol (DTT) and cysteine. This sets PCB/CBX-SS hydrogels apart from nondegradable gels for drug delivery applications: its drug release behavior should be convenient for modulation via reductants. Therefore, we evaluated the in vitro release profile of FITC-conjugated bovine serum albumin (FITC-BSA) from a PCB/CBX-SS hydrogel in different DTT concentrations to explore its utility as a drug release system. Figure 4 tracks the cumulative release of FITC-BSA over time under reducing and nonreducing conditions. In PBS without DTT, following an initial burst release in the first hour, sustained release was observed, and a relatively low cumulative release of about 42% was achieved after 8 h. When the hydrogels were instead immersed in a 5 mM DTT solution, the rapid initial release over the first 2 h was enhanced, showing a nearly linear trend. As disulfide bonds continued to break, cumulative FITC-BSA release increased over the next 6 h but at a relatively lower rate. A similar trend was observed when we increased the DTT concentration to 20 mM, and as much as 89% of the total FITC-BSA was released after 8 h. These results suggest that PCB/CBX-SS hydrogels may have the potential to act as a controllable drug release system.

3.6. Immunogenicity Mitigation by Degradable PCB/CBX-SS Nanocages. Protein therapeutics possessing high specificity and low immunogenicity are increasingly used to treat diseases such as cancer, diabetes, cardiovascular disease, inflammation, multiple sclerosis, arthritis, and infectious diseases. However, the efficacy of protein drugs is limited by in vivo instability, immunogenicity, and relatively short circulating half-lives. ^{19–22} Conjugating PEG to these proteins (PEGylation) has been the most successful strategy for addressing these problems. However, there have been increasing reports connecting the generation of anti-PEG antibodies with bioactivity loss and increased adverse effects after frequent administration of PEGylated therapies. ^{23–25} Recently, our group has developed zwitterionic PCB nanogels

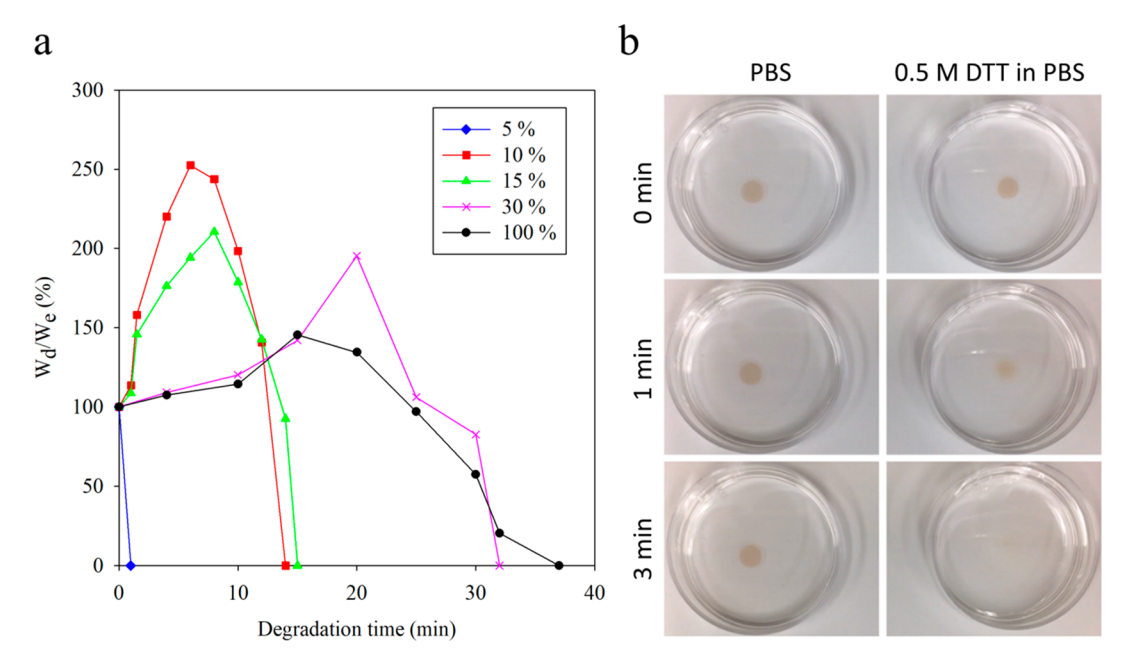


Figure 3. (a) Weight changes of hydrated PCB/CBX-SS hydrogels with different cross-linker amounts in 100 mM DTT solution in PBS at room temperature. (b) Degradation of PCB/CBX-SS hydrogels with 15 mol % cross-linker in PBS and PBS containing 0.5 M DTT, respectively.

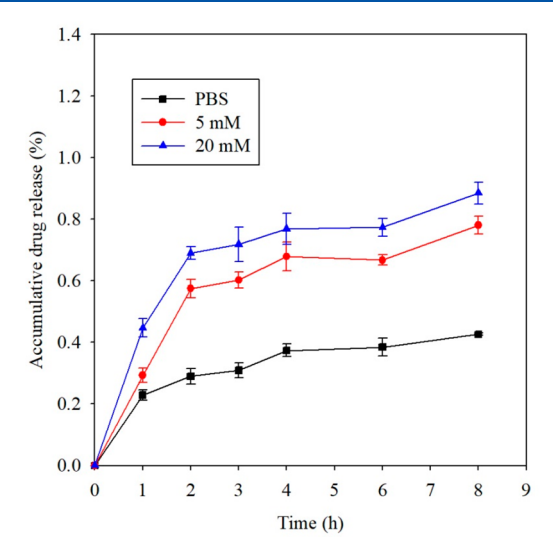


Figure 4. Release profile of FITC-conjugated bovine serum albumin (FITC-BSA) from a PCB/CBX-SS hydrogel with a 10% cross-linking ratio by mole in PBS, 5 mM DTT, and 20 mM DTT solutions.

and nanocages to protect proteins, improving their stability as well as immunological and pharmacokinetic properties. 10,15,26 Both of these approaches have used nanocarriers composed of cross-linked zwitterionic PCB backbones that are not degradable. However, the degradation of nanocarriers into low molar mass components is highly desirable for improving clearance via renal filtration. Previously, our group demonstrated that the encapsulation of uricase, a highly immunogenic enzyme, in nondegradable PCB NCs induces no antiuricase or anti-PCB antibodies following repeated administration of the drug. 15 To determine whether incorporating a degradable cross-linker in PCB NCs hampers its capacity to eliminate undesirable immune responses, we herein prepared degradable zwitterionic PCB NCs using the CBX-SS cross-linker. These NCs were prepared following the protocol reported by Li et al. Repetitive IV injections of native uricase and PCB-NC-

encapsulated uricase (PCB-uricase) were performed on healthy Sprague-Dawley rats. After 3 weeks, blood was drawn and rat sera were collected for antibody detection. While a strong antiprotein (antiuricase) antibody response was observed in the native uricase group, no detectable IgM or IgG against either uricase or PCB was observed in the group treated with degradable PCB-uricase NCs, as shown in Figure 5. Also, as presented in Figure 6, PCB NCs significantly enhanced the circulation time of uricase 10-fold compared to that of the native protein. This long circulation time resulted from both the nonfouling property and low degradation of PCB NCs. The concentration of GSH in rat blood is only 22-27 μ M while that in cells is 1-2 mM. Under the circumstance of a low reductant level in blood, the half-life of nanocage degradation during circulation is expected to be long. In contrast, the degradation of a nanocage engulfed by cells would be expedited due to the presence of a highly concentrated reductant in cells. At the cross-linker ratio used in this work, nanocage degradation in cells is expected to be complete within 12 h. Therefore, we expect that nanocages made from CBX-SS would be stable in the blood for long circulation times, avoiding premature release, but would end up being degraded after cell uptake.

4. CONCLUSIONS

We synthesized a degradable cross-linker, CBX-SS, containing both zwitterionic carboxybetaine units and a disulfide linkage. The synthesis route of CBX-SS is simple and robust and can be readily scaled up to produce larger quantities. PCB hydrogels cross-linked with CBX-SS exhibited excellent nonfouling properties and degradability. We found encapsulated FITC-BSA to be effectively released from PCB/CBX-SS hydrogels in vitro. Furthermore, we showed the applicability of CBX-SS in producing degradable PCB nanocages to encapsulate a highly immunogenic enzyme, uricase. These PCB/CBX-SS nanocages eliminated or prevented immune responses toward both the protein and polymer. Degradable zwitterionic biomaterials

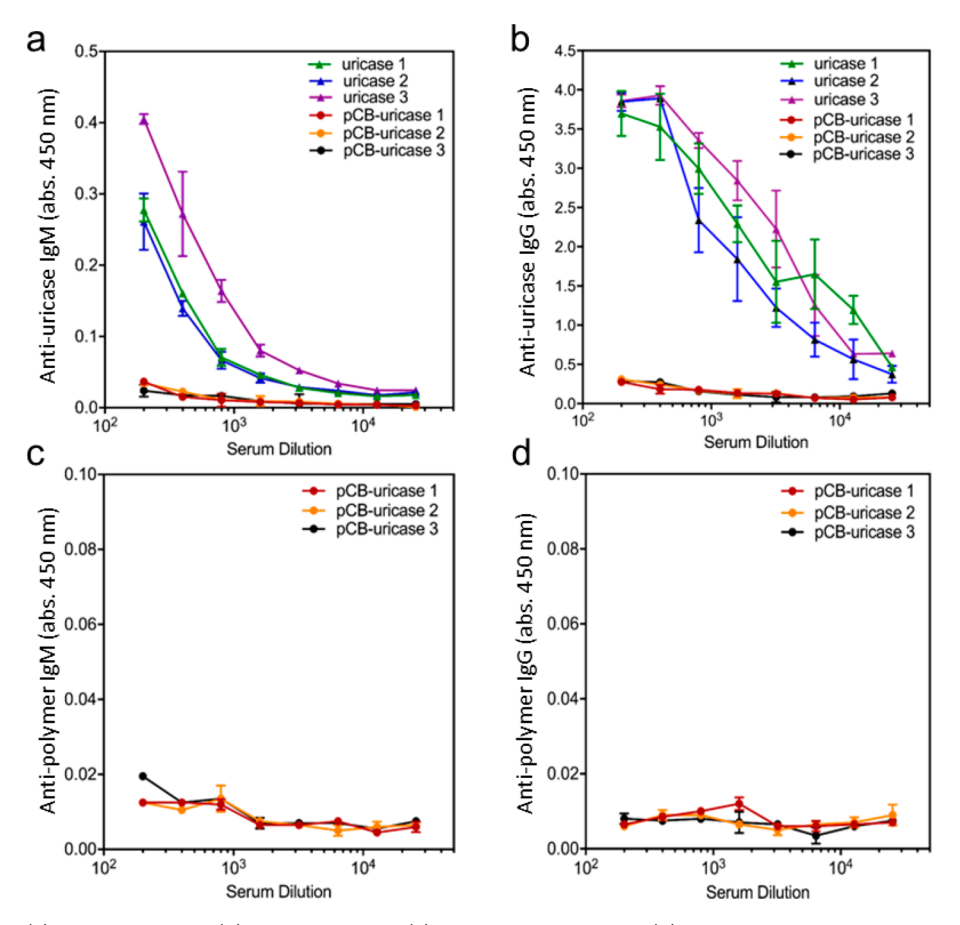


Figure 5. Detection of (a) antiuricase IgM, (b) antiuricase IgG, (c) antipolymer IgM, and (d) antipolymer IgG in rat sera collected 21 days after the injection of native uricase and PCB NC.

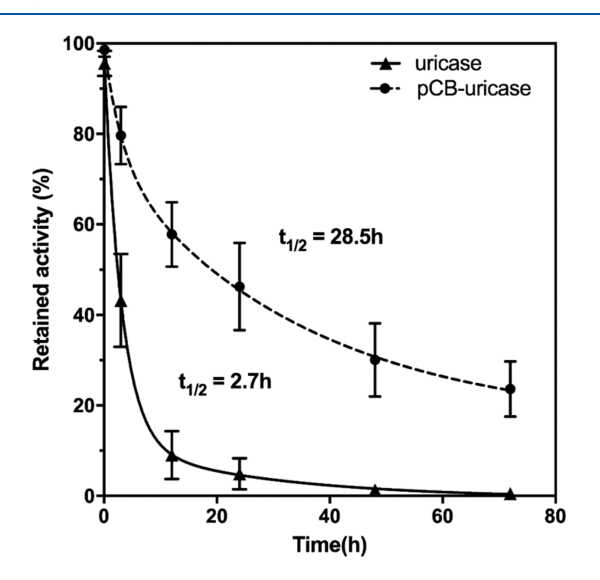


Figure 6. Circulation profile of native uricase and uricase encapsulated in degradable PCB NCs.

made with CBX-SS are promising for a wide range of drug delivery and tissue engineering applications.

AUTHOR INFORMATION

Corresponding Author

*E-mail: sjiang@uw.edu.

ORCID

Xiaojie Lin: 0000-0003-2911-3685 Peng Zhang: 0000-0002-5409-7480 Shaoyi Jiang: 0000-0001-9863-6899

Author Contributions

§These authors contributed equally.

Notes

The authors declare the following competing financial interest(s): Dr. Shaoyi Jiang is a cofounder of Taproot Medical Technologies LLC.

ACKNOWLEDGMENTS

This work was supported by the Office of Naval Research (N00014-16-1-3084), the Defense Threat Reduction Agency (HDTRA1-13-1-0044), the National Science Foundation (DMR 1708436), and the University of Washington.

REFERENCES

- (1) Venault, A.; Hsu, C.-H.; Ishihara, K.; Chang, Y. Zwitterionic bicontinuous membranes from a phosphobetaine copolymer/poly-(vinylidene fluoride) blend via VIPS for biofouling mitigation. *J. Membr. Sci.* **2018**, *550*, 377–388.
- (2) Dizon, G. V.; Venault, A. Direct in-situ modification of PVDF membranes with a zwitterionic copolymer to form bi-continuous and fouling resistant membranes. *J. Membr. Sci.* **2018**, *550*, 45–58.
- (3) Zhang, Y.; Chen, W.; Yang, C.; Fan, Q.; Wu, W.; Jiang, X. Enhancing tumor penetration and targeting using size-minimized and zwitterionic nanomedicines. *J. Controlled Release* **2016**, 237, 115–124.

(4) Zhu, Y.; Zhang, J.; Yang, J.; Pan, C.; Xu, T.; Zhang, L. Zwitterionic hydrogels promote skin wound healing. *J. Mater. Chem. B* **2016**, *4*, 5105–5111.

- (5) Qi, H.; Du, Y.; Hu, G.; Zhang, L. Poly(carboxybetaine methacrylate)-functionalized magnetic composite particles: A biofriendly support for lipase immobilization. *Int. J. Biol. Macromol.* **2018**, 107. 2660–2666.
- (6) Wang, G.; Wang, L.; Lin, W.; Wang, Z.; Zhang, J.; Ji, F.; Ma, G.; Yuan, Z.; Chen, S. Development of Robust and Recoverable Ultralow-Fouling Coatings Based on Poly(carboxybetaine) Ester Analogue. ACS Appl. Mater. Interfaces 2015, 7, 16938–16945.
- (7) Cao, B.; Tang, Q.; Cheng, G. Recent advances of zwitterionic carboxybetaine materials and their derivatives. *J. Biomater. Sci., Polym. Ed.* **2014**, 25, 1502–1513.
- (8) Zhang, L.; Cao, Z.; Bai, T.; Carr, L.; Ella-Menye, J.-R.; Irvin, C.; Ratner, B. D.; Jiang, S. Zwitterionic hydrogels implanted in mice resist the foreign-body reaction. *Nat. Biotechnol.* **2013**, *31*, 553.
- (9) Bai, T.; Sun, F.; Zhang, L.; Sinclair, A.; Liu, S.; Ella-Menye, J. R.; Zheng, Y.; Jiang, S. Restraint of the Differentiation of Mesenchymal Stem Cells by a Nonfouling Zwitterionic Hydrogel. *Angew. Chem., Int. Ed.* **2014**, *53*, 12729–12734.
- (10) Zhang, P.; Sun, F.; Tsao, C.; Liu, S.; Jain, P.; Sinclair, A.; Hung, H.-C.; Bai, T.; Wu, K.; Jiang, S. Zwitterionic gel encapsulation promotes protein stability, enhances pharmacokinetics, and reduces immunogenicity. *Proc. Natl. Acad. Sci. U. S. A.* **2015**, *112*, 12046–12051.
- (11) Carr, L. R.; Xue, H.; Jiang, S. Functionalizable and nonfouling zwitterionic carboxybetaine hydrogels with a carboxybetaine dimethacrylate crosslinker. *Biomaterials* **2011**, 32, 961–968.
- (12) Lyu, S.; Untereker, D. Degradability of Polymers for Implantable Biomedical Devices. *Int. J. Mol. Sci.* **2009**, *10*, 4033–4065.
- (13) Meng, F.; Hennink, W. E.; Zhong, Z. Reduction-sensitive polymers and bioconjugates for biomedical applications. *Biomaterials* **2009**, *30*, 2180–2198.
- (14) Zhang, L.; Xue, H.; Cao, Z.; Keefe, A.; Wang, J.; Jiang, S. Multifunctional and degradable zwitterionic nanogels for targeted delivery, enhanced MR imaging, reduction-sensitive drug release, and renal clearance. *Biomaterials* **2011**, 32, 4604–4608.
- (15) Li, B.; Yuan, Z.; Zhang, P.; Sinclair, A.; Jain, P.; Wu, K.; Tsao, C.; Xie, J.; Hung, H. C.; Lin, X.; Bai, T.; Jiang, S. Zwitterionic Nanocages Overcome the Efficacy Loss of Biologic Drugs. *Adv. Mater.* **2018**, *30*, 1705728.
- (16) Li, B.; Xie, J.; Yuan, Z.; Jain, P.; Lin, X.; Wu, K.; Jiang, S. Mitigation of Inflammatory Immune Responses with Hydrophilic Nanoparticles. *Angew. Chem., Int. Ed.* **2018**, *57*, 4527–4531.
- (17) Huglin, M. B.; Rego, J. M. Influence of temperature on swelling and mechanical properties of a sulphobetaine hydrogel. *Polymer* **1991**, 32, 3354–3358.
- (18) Zhang, Z.; Chao, T.; Jiang, S. Physical, Chemical, and Chemical–Physical Double Network of Zwitterionic Hydrogels. *J. Phys. Chem. B* **2008**, *112*, 5327–5332.
- (19) De Groot, A. S.; Scott, D. W. Immunogenicity of protein therapeutics. *Trends Immunol.* **2007**, 28, 482–490.
- (20) Kromminga, A.; Schellekens, H. Antibodies against Erythropoietin and Other Protein-Based Therapeutics: An Overview. *Ann. N. Y. Acad. Sci.* **2006**, *1050*, 257–265.
- (21) Kontermann, R. E. Strategies for extended serum half-life of protein therapeutics. *Curr. Opin. Biotechnol.* **2011**, *22*, 868–876.
- (22) Nagata, S.; Pastan, I. Removal of B cell epitopes as a practical approach for reducing the immunogenicity of foreign protein-based therapeutics. *Adv. Drug Delivery Rev.* **2009**, *61*, 977–985.
- (23) Leger, R. M.; Arndt, P.; Garratty, G.; Armstrong, J.; Meiselman, H. J.; Fisher, T. Normal donor sera can contain antibodies to polyethylene glycol (PEG). *Transfusion* **2001**, *41*, 29S.
- (24) Armstrong, J.; Leger, R.; Wenby, R.; Meiselman, H. J.; Garratty, G.; Fisher, T. Occurrence of an antibody to poly(ethylene glycol) in normal donors. *Blood* **2003**, *102*, 556A.

(25) Garratty, G. Progress in modulating the RBC membrane to produce transfusable universal/stealth donor RBCs. *Transfusion Medicine Reviews* **2004**, *18*, 245–256.

(26) Zhang, P.; Jain, P.; Tsao, C.; Sinclair, A.; Sun, F.; Hung, H.-C.; Bai, T.; Wu, K.; Jiang, S. Butyrylcholinesterase nanocapsule as a long circulating bioscavenger with reduced immune response. *J. Controlled Release* **2016**, 230, 73–78.